

Syntheses of the $(\text{Nd}_x, \text{Sm}_{1-x})\text{AlO}_3$ and Its Structure Relation to a Series of Rare Earth Orthoaluminates RAIO_3

Akira Yoshikawa,^{*1} Hiroyuki Horiuchi,^{*2} Masahiko Tanaka,[†] Toetsu Shishido,[‡] and Tsuguo Fukuda[‡]

^{*}Mineralogical Institute, Graduate School of Science, University of Tokyo, 7-3-1 Hongo, Bunkyo-ku, Tokyo 113, Japan; [†]Photon Factory, National Laboratory for High Energy Physics, Oho, Tsukuba, Ibaragi 305, Japan; and [‡]Institute for Materials Research, Tohoku University, 2-1-1 Katahira, Aoba-ku, Sendai 980, Japan

Received July 20, 1995; in revised form June 11, 1996; accepted July 23, 1996

Structure change from orthorhombic to trigonal system of $(\text{Nd}_x, \text{Sm}_{1-x})\text{AlO}_3$, which takes place by substituting Sm^{3+} for Nd^{3+} , was investigated by X-ray powder diffraction method. The samples were prepared by a solid state reaction. Their structures are based on a perovskite-type structure with slightly deformed lattices from an ideal cubic structure. The lattice deformation from an ideal cubic lattice is minimum at around $x = 0.0$ and it systematically increases by the amount of substitution of Sm^{3+} for Nd^{3+} , and the structure changes from orthorhombic to trigonal system at around $x = 0.7$. Thus, the substitution of Sm^{3+} for Nd^{3+} apparently plays a role of the changes of temperature and/or pressure for the cause of a first-order phase transition. © 1996 Academic Press, Inc.

1. INTRODUCTION

A series of rare earth orthoaluminates, RAIO_3 , belongs to one of the typical groups of perovskite-type structures. Geller and Bala (1) determined the lattice constants of RAIO_3 for $R = \text{La}, \text{Pr}, \text{Nd}, \text{Sm}, \text{Eu},$ and Gd by powder X-ray diffraction. They concluded that RAIO_3 for $R = \text{La}, \text{Pr},$ and Nd are trigonal with a rhombohedral lattice, and other three phases are orthorhombic as a result. Dernier and Maines (2) synthesized orthorhombic phases for RAIO_3 with $R = \text{Sm}–\text{Lu}$ under the conditions of 32.5 kbar and 1200°C using NaOH as a flux. Recently, Shishido *et al.* (3, 4) prepared all of the phases of RAIO_3 for $R = \text{La}–\text{Lu}$ under ambient pressure by the flux method using KF as a solvent, and determined their lattice constants by powder X-ray diffraction. As a conclusion of these works, the relationship among the lattice vectors of RAIO_3 and an ideal cubic structure is summarized as follows:

$$\begin{aligned} \mathbf{a}_t &= \mathbf{a}_1 + \mathbf{a}_2, & \mathbf{b}_t &= \mathbf{a}_2 + \mathbf{a}_3, & \mathbf{c}_t &= \mathbf{a}_3 + \mathbf{a}_1; \\ & & & & & \text{for trigonal (rhombohedral) phases,} \\ \mathbf{a}_o &= \mathbf{a}_1 + \mathbf{a}_3, & \mathbf{b}_o &= 2 \cdot \mathbf{a}_2, & \mathbf{c}_o &= \mathbf{a}_1 - \mathbf{a}_3; \\ & & & & & \text{for orthorhombic phases,} \end{aligned}$$

where $\mathbf{a}_t, \mathbf{b}_t, \mathbf{c}_t$ and $\mathbf{a}_o, \mathbf{b}_o, \mathbf{c}_o$ are lattice vectors for trigonal and orthorhombic lattices of RAIO_3 , respectively, and $\mathbf{a}_1, \mathbf{a}_2,$ and \mathbf{a}_3 , are those for an ideal cubic perovskite-type structure which is used as a “basic lattice” in this work. These relations are schematically shown in Fig. 1.

An interesting feature of a series of these structures is that the lattice parameters systematically change against the ionic radius of R , and that the structures of RAIO_3 with smaller atomic numbers of La–Nd crystallize in the trigonal system, while, those with larger atomic numbers of Sm–Lu show orthorhombic structures. CeAlO_3 is only exceptional and most works report that it is tetragonal (5–8), however, Kim (9) reported it to be rhombohedral.

It will be of interest to note what ionic radius is the critical size for the structure to change from orthorhombic to trigonal and how the structure change takes place at the point. In this study, we tried to synthesize solid solution phases of $(\text{Nd}_x, \text{Sm}_{1-x})\text{AlO}_3$ in the $\text{NdAlO}_3–\text{SmAlO}_3$ system, and the substitution effects of Sm for Nd on the crystal structures were investigated in order to imply the phase transition mechanism of RAIO_3 as a kind of chemical simulation.

2. EXPERIMENTS

2.1. Sample Preparation of $\text{NdAlO}_3–\text{SmAlO}_3$ Solid Solution

Six kinds of samples with the chemical composition of $(\text{Nd}_x, \text{Sm}_{1-x})\text{AlO}_3$ with $x = 0.0, 0.2, 0.4, 0.6, 0.8,$ and 1.0 were prepared by solid state reaction. Commercial re-

¹ Present address: Department of Superconductivity, Graduate School of Engineering, University of Tokyo, 7-3-1 Hongo, Bunkyo-ku, Tokyo 113, Japan.

² To whom correspondence should be addressed.

TABLE 1a
Experimental Conditions of Powder X-Ray Diffraction

X-ray source: $\text{CuK}\alpha$ from shield tube, 35 kV and 22.5 mA, with analyzer monochromator of pyrolytic graphite (002)
Measured range and scan method: $2\theta = 5^\circ\text{--}85^\circ$, $\theta - 2\theta$ scan, $0.02^\circ/\text{step}$ for 2θ , 20 sec/step
Optical system: 1° for both divergence and scattering slits, 0.2 mm for receiving slit.
Apparatus: JDX8020/Jeol

agents Nd_2O_3 and Sm_2O_3 with purification of 99.99% and Al_2O_3 with that of 99.999% (High Purity Chemicals Co. Ltd.) were used as the starting materials. Their mixtures with the appropriate composition were heated

up to 1600°C at the rate of $1000^\circ\text{C}/\text{h}$, held for 2 h at that temperature, and cooled down to room temperature at the rate of $700^\circ\text{C}/\text{h}$. A high frequency induction furnace was used, and the reaction was performed using a graphite crucible under He gas atmosphere. The obtained products were polycrystals with particle sizes of less than $3\ \mu\text{m}$.

2.2. Phase Identification by Powder X-Ray Diffraction

Synthetic products were examined by powder X-ray diffraction. The experimental conditions are summarized in Table 1a. Their patterns are shown in Figs. 2a and 2b.

The peak positions of each diffraction pattern were carefully analyzed by a peak decomposition program (10). An example of the results of a peak decomposition is shown in Fig. 2c for the reflections of 301 and 103 of the phase with $x = 0.4$. In fact, they are not only 301 and 103 reflections but also 222 and 141 reflections are included in this profile as shown in Table 1b. These analyses are necessary for the separation of nearly overlapped peaks which are due to a very small lattice deformation from the basic lattice. The comparison of d_{obs} and d_{calc} and the lattice parameters refined by the least-squares refinements are listed in Tables 1b and 1c. It was difficult to determine precise chemical compositions of the products by an electron probe microanalysis because of too small crystal particles. However, each diffraction pattern of Fig. 2 could be indexed by a single phase without any observable mixtures, therefore, their chemical compositions were assumed to be the same as their starting compositions. In fact, the lattice parameters systematically change depending on the assumed chemical compositions, as discussed later.

3. RESULTS AND DISCUSSION

3.1. Experimental Results of $\text{NdAlO}_3\text{--SmAlO}_3$

As a result of phase analyses by powder X-ray diffraction, it was found that $(\text{Nd}_x, \text{Sm}_{1-x})\text{AlO}_3$ with $x = 0.0\text{--}0.6$ belongs to the orthorhombic phase, and those with $x = 0.8\text{--}1.0$ are trigonal phases with a rhombohedral lattice. This result suggests that the structure of $(\text{Nd}_x, \text{Sm}_{1-x})\text{AlO}_3$ changes from orthorhombic to trigonal at the chemical composition between $x = 0.6$ and 0.8 , that is, at the ionic radius of around $0.97\ \text{\AA}$. The relationship between the chemical compositions and lattice constants obtained in this work was plotted in Fig. 3a and its relation to a series of RAlO_3 ($R = \text{La--Lu}$) (3) was also plotted in Fig. 3b. Thus, $(\text{Nd}_x, \text{Sm}_{1-x})\text{AlO}_3$ are structurally classified into two groups and the lattice constants obey Vegard's law in each structure group as shown in Fig. 3a.

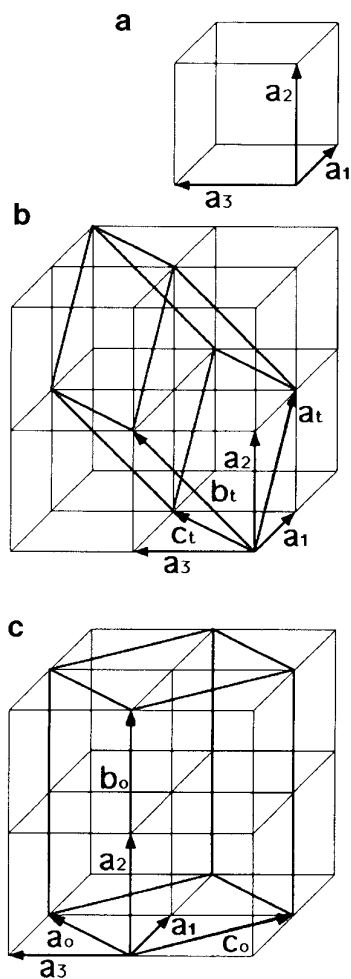


FIG. 1. Lattice relationship between an ideal cubic perovskite-type lattice (thin real lines), and rhombohedral and orthorhombic lattices (bold real lines). (a) Lattice corresponding to an ideal cubic perovskite-type structure. This lattice is assigned as a "basic lattice" in text. (b) Rhombohedral lattice. (c) Orthorhombic lattice.

TABLE 1b
 Comparison d_{obs} and d_{calc} for (Nd_x, Sm_{1-x})AlO₃. Reflections with d_{obs} Values Were Obtained by Analyses of Peak Decomposition. Reflections in the 2θ Range of 0–72° and 0–80° Are Listed in the Table for Orthorhombic and Rhombohedral Phases, Respectively, and Reflections in the Range of 0–80° Were Used for the Determination of Lattice Constants of Their Phases

			Orthorhombic phases						Rhombohedral phases					
			SmAlO ₃		(Nd _{0.2} ,Sm _{0.8})AlO ₃		(Nd _{0.4} ,Sm _{0.6})AlO ₃		(Nd _{0.6} ,Sm _{0.4})AlO ₃		(Nd _{0.8} ,Sm _{0.2})AlO ₃		NdAlO ₃	
<i>h</i>	<i>k</i>	<i>l</i>	d_{obs}	d_{calc}	d_{obs}	d_{calc}	d_{obs}	d_{calc}	d_{obs}	d_{calc}	d_{obs}	d_{calc}	d_{obs}	d_{calc}
1	0	1	3.7366	3.7378	3.7479	3.7430	3.7466	3.7459	3.7536	3.7494	3.7538	3.7500	3.7549	3.7513
0	2	0	3.7345	3.7345	3.7390	3.7390	3.7355	3.7355	3.7430	3.7430	2.6608	2.6600	2.6618	2.6605
1	1	1	3.3427	3.3426	3.3499	3.3471	3.3514	3.3486	3.3539	3.3524	2.6525	2.6434	2.6534	2.6448
2	0	0	2.6490	2.6440	2.6516	2.6478	2.6472	2.6515	2.6596	2.6554	2.2630	2.2626	2.2628	2.2634
0	0	2	2.6404	2.6420	2.6472	2.6456	2.6460	2.6460	2.6470	2.6470	2.1697	2.1696	2.1707	2.1701
1	2	1	2.6418	2.6418	2.6453	2.6453	2.6451	2.6451	2.6490	2.6490	2.2	2	2.1532	2.1531
2	1	0	2.4956	2.4924	2.4946	2.4941	2.4964	2.4988	2.4964	2.4988	0	2	1.8750	1.8750
0	1	2	2.4908	2.4908	2.4940	2.4940	2.4942	2.4942	2.4942	2.4942	-1	1	1.6814	1.6812
0	3	0	2.4897	2.4897	2.4927	2.4927	2.4903	2.4903	2.4903	2.4903	1	2	1.6763	1.6729
2	1	1	2.2532	2.2542	2.2594	2.2574	2.2584	2.2574	2.1648	2.1622	-1	1	1.5357	1.5357
2	1	2	2.2511	2.2533	2.2564	2.2564	2.2564	2.2564	2.1679	2.1657	0	1	1.5324	1.5325
2	2	0	2.1591	2.1579	2.1632	2.1609	2.1632	2.1609	2.1611	2.1611	2	3	1.5226	1.5230
0	2	2	2.1530	2.1568	2.1602	2.1597	2.1599	2.1592	2.1678	1.8747	-2	0	1.3298	1.3300
2	0	2	1.8678	1.8689	1.8722	1.8715	1.8736	1.8730	1.8753	1.8747	2	2	1.3213	1.3217
0	4	0	1.8673	1.8673	1.8700	1.8700	1.8678	1.8678	1.8715	1.8714	-1	0	1.2540	1.2537
2	1	2	1.8127	1.8130	1.8155	1.8155	1.8155	1.8155	1.6778	1.6766	1	1	1.2507	1.2504
2	3	0	1.8126	1.8126	1.8163	1.8150	1.8163	1.8150	1.6743	1.6743	3	3	1.2439	1.2439
0	3	2	1.8119	1.8119	1.8142	1.8142	1.8142	1.8142	1.6740	1.6738	-1	2	1.1880	1.1884
3	0	1	1.6736	1.6721	1.6769	1.6745	1.6778	1.6766	1.6805	1.6789	1	3	1.1832	1.1842
2	2	2	1.6713	1.6713	1.6736	1.6736	1.6736	1.6736	1.6751	1.6746	0	2	1.1880	1.1881
1	0	3	1.6689	1.6711	1.6734	1.6734	1.6740	1.6738	1.6751	1.6746	1	10	1.1832	1.1836
1	4	1	1.6704	1.6704	1.6725	1.6725	1.6715	1.6715	1.6745	1.6745	1	11	1.1832	1.1836
3	1	1	1.6327	1.6317	1.6329	1.6340	1.6329	1.6359	1.6329	1.6359	0	2	1.5328	1.5319
1	1	3	1.6308	1.6308	1.6329	1.6329	1.6333	1.6333	1.5328	1.5319	1	12	1.5283	1.5286
3	2	1	1.5266	1.5261	1.5291	1.5282	1.5308	1.5296	1.5277	1.5275	1	18	1.5283	1.5286
1	2	3	1.5228	1.5253	1.5275	1.5274	1.5277	1.5275	1.5277	1.5275	1	18	1.5283	1.5286
2	4	0	1.5252	1.5252	1.5273	1.5273	1.5273	1.5273	1.5270	1.5270	1	18	1.5283	1.5286
0	4	2	1.5246	1.5246	1.5268	1.5268	1.5259	1.5259	1.5281	1.5281	1	18	1.5283	1.5286
2	3	2	1.4938	1.4946	1.4946	1.4946	1.4946	1.4946	1.3892	1.3908	1	13	1.3289	1.3277
0	5	0	1.4938	1.4938	1.3891	1.3900	1.3892	1.3908	1.3289	1.3277	1	13	1.3289	1.3277
3	3	1	1.3881	1.3881	1.3893	1.3893	1.3893	1.3893	1.3235	1.3230	1	9	1.3235	1.3230
1	3	3	1.3875	1.3875	1.3888	1.3888	1.3879	1.3879	1.3225	1.3225	1	9	1.3225	1.3225
1	5	1	1.3871	1.3871	1.3888	1.3888	1.3879	1.3879	1.3268	1.3258	1	9	1.3268	1.3258
4	0	0	1.3234	1.3220	1.3250	1.3239	1.3250	1.3239	1.3235	1.3230	1	13	1.3235	1.3230
0	0	4	1.3196	1.3210	1.3230	1.3228	1.3230	1.3228	1.3225	1.3225	1	13	1.3225	1.3225
2	4	2	1.3209	1.3209	1.3227	1.3227	1.3225	1.3225	1.3225	1.3225	1	13	1.3225	1.3225

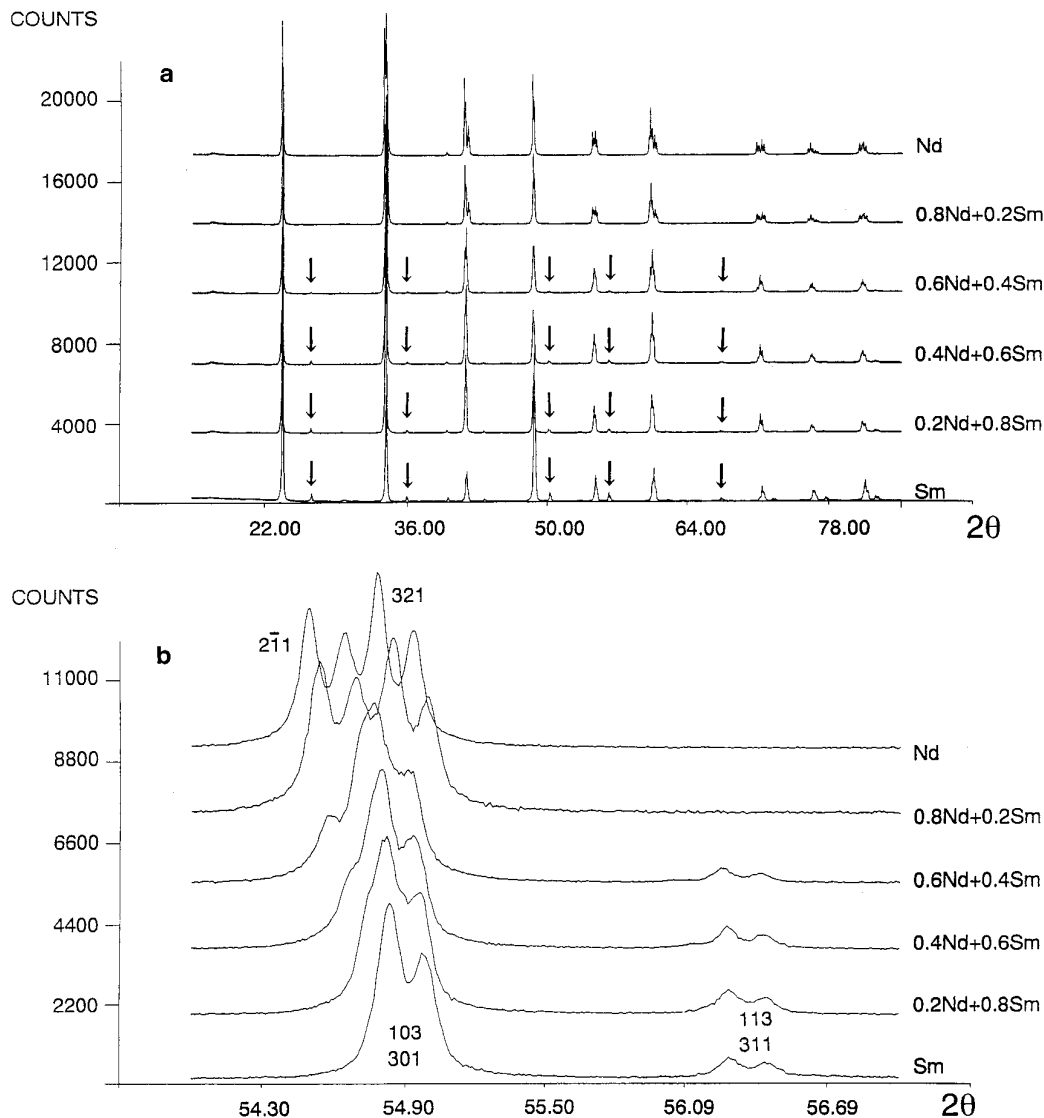


FIG. 2. (a) Comparison of powder X-ray diffraction patterns of $(\text{Nd}_x, \text{Sm}_{1-x})\text{AlO}_3$ for $x = 0.0, 0.2, 0.4, 0.6, 0.8,$ and 1.0 . Strong reflection peaks are similar over all phases, however weak reflection peaks designated by arrows are observed only in the phases with $x = 0.0-0.6$. (b) Parts of diffraction patterns of $(\text{Nd}_x, \text{Sm}_{1-x})\text{AlO}_3$. Patterns clearly show the structure change at the chemical composition between $x = 0.6$ and 0.8 . (c) Examples of profile fitting analyses for 2θ range of $53.85^\circ-55.85^\circ$. Reflections of 103 and 301 of orthorhombic phase with $x = 0.4$ are almost overlapped.

3.2. Discussion of Structure Change in $(\text{Nd}_x, \text{Sm}_{1-x})\text{AlO}_3$

A slight difference of ionic radii in the structure of $(\text{Nd}_x, \text{Sm}_{1-x})\text{AlO}_3$, which is realized by the partial substitution of Sm^{3+} (0.95 \AA) for Nd^{3+} (0.98 \AA) (11), affects on the degree of the lattice deformation and on the atomic positions of R and oxygen. Weak reflection peaks which are shown by arrows in Fig. 2a will be caused by the atomic shift from the ideal cubic structure, however, they will mainly be attributed to the shift of the R atom because of its much larger atomic scattering factor than that of the

oxygen atom. Al atoms do not contribute to these structure factors because of their special positions. The magnitudes of their intensities gradually decrease depending on the increase of the value of x , and finally have not been observed at $x = 0.8$. That is, R atom positions turn out to be at an ideal position at around $x = 0.7$.

On the other hand, the difference between the values of a and c ($\text{Nd}_x, \text{Sm}_{1-x})\text{AlO}_3$ is smallest at $x = 0.0$, which corresponds to the composition of SmAlO_3 . The difference of their values becomes larger when the value of x increases by substitution of Sm^{3+} for Nd^{3+} , that is,

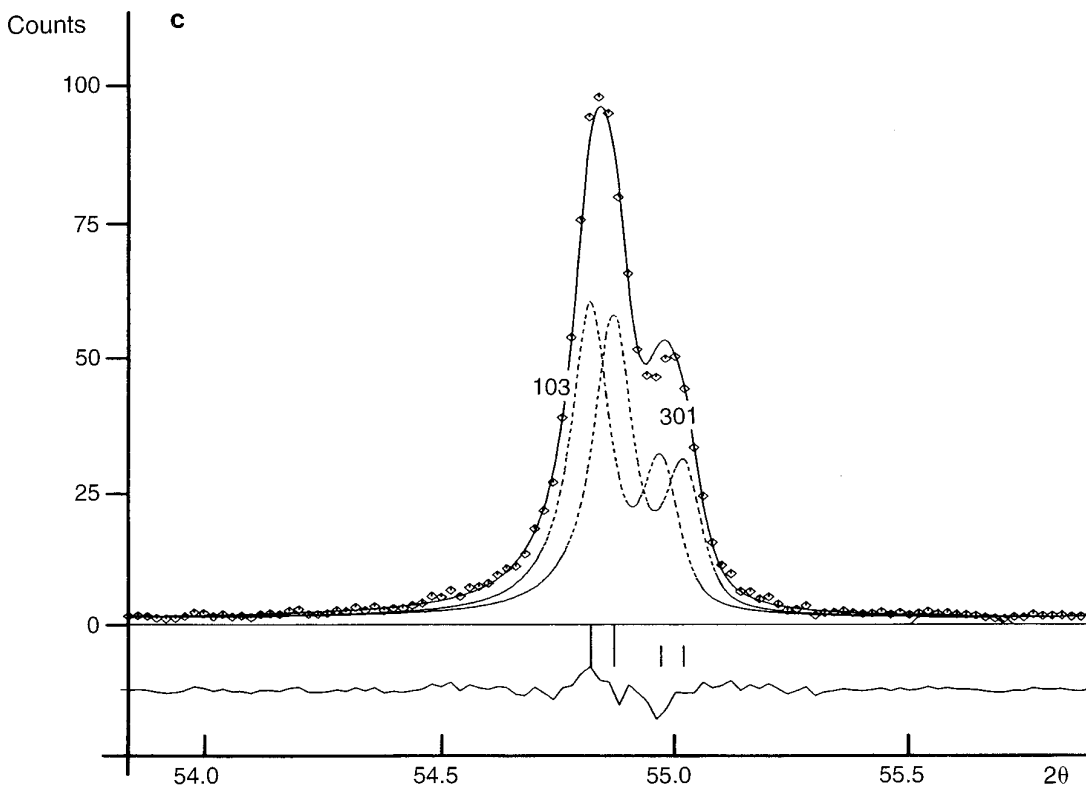


FIG. 2—Continued

by the replacement of a smaller rare-earth ion by a larger one. Thus, the lattice deformation becomes smallest at around $x = 0.0$ against the magnitude of the shift of atomic positions.

From these observed results, it will be concluded that the structure change of (Nd_x, Sm_{1-x})AlO₃ from orthorhombic to trigonal, which is caused by the ionic substitution, does not pass an intermediate structure, such as an ideal cubic structure, but it directly changes from orthorhombic to trigonal at around $x = 0.7$. The phase transition of SmAlO₃ from orthorhombic to trigonal at high tempera-

tures was observed by O'Bryan *et al.* (13). It is of interest to note that the structure change observed by substituting Sm³⁺ for Nd³⁺ shows a similar behavior to the phase transition of SmAlO₃ which takes place by changing temperatures.

As a conclusion, the existence of two structure types of solid solution phases of (Nd_x, Sm_{1-x})AlO₃ was confirmed in the SmAlO₃-NdAlO₃ system. The substitution of Sm³⁺ for Nd³⁺ effects cause a structure change from the orthorhombic to the trigonal system at the chemical composition of around (Nd_{0.7}, Sm_{0.3})AlO₃ like a first-order phase transition which takes place by changing temperature and/or pressure.

TABLE 1c

Lattice Constants of (Nd_x, Sm_{1-x})AlO₃ Determined by Least-Squares Refinements (11) Based on the Values in Table 1b

x	a	b	c	α	Cell volume	Molar volume	Crystal system
0.0	5.288(1)	7.469(2)	5.284(1)	—	208.7(1)	52.18	Ortho.
0.2	5.296(1)	7.478(5)	5.291(1)	—	209.5(1)	52.37	Ortho.
0.4	5.303(1)	7.471(3)	5.292(1)	—	209.6(1)	52.40	Ortho.
0.6	5.311(1)	7.486(5)	5.294(1)	—	210.4(1)	52.60	Ortho.
0.8	5.287(2)	—	—	60.41(2)	105.5(2)	52.75	Trig.
1.0	5.290(3)	—	—	60.39(4)	105.6(3)	52.80	Trig.

ACKNOWLEDGMENTS

The authors are grateful to Mr. R. Note of the Institute for Materials Research, Tohoku University for his help on the syntheses of the samples, and Mr. O. Tachikawa, Mr. A. Saito, and Mr. G. Zou of the Mineralogical Institute, University of Tokyo for their help on the EDS and powder X-ray analyses. Authors HH and TS were supported by Grant-in Aid for Scientific Research of (B)-07459008 and (PA)-06241107 of The Ministry of Education, Science and Culture of Japanese Government, respectively, and this work was performed under the Inter-University Cooperative Research Program of the Institute for Materials Research, Tohoku University.

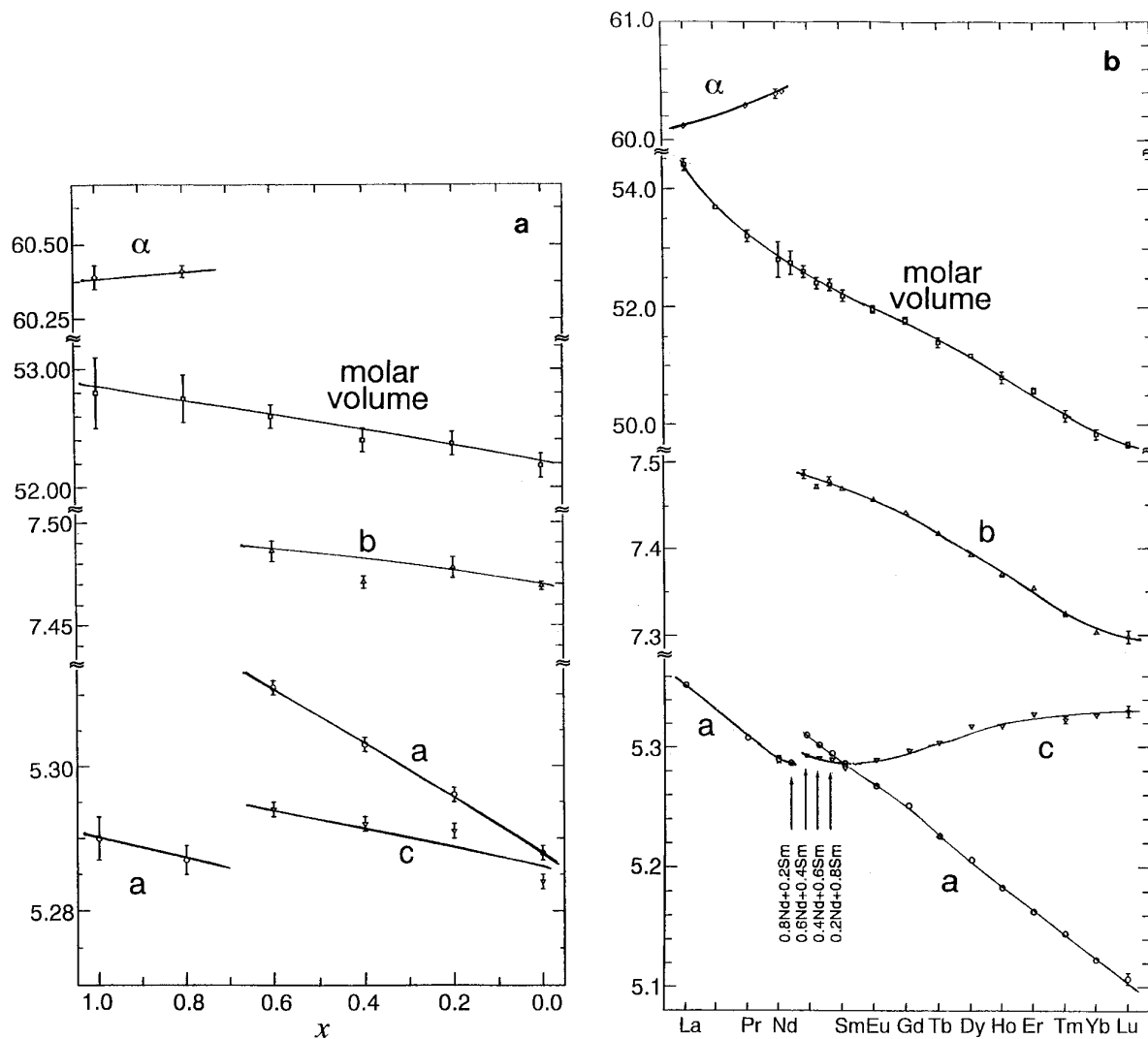


FIG. 3. (a) Plot of lattice constants of the phases $(\text{Nd}_x, \text{Sm}_{1-x})\text{AlO}_3$. The phases of $x = 0-0.6$ are orthorhombic and those of $x = 0.8-1.0$ are trigonal with rhombohedral lattice. (b) The change of lattice constants of a series of RAlO_3 and its relation to those of the phases $(\text{Nd}_x, \text{Sm}_{1-x})\text{AlO}_3$. The values of a and c cross at around SmAlO_3 . The lattice constants of a series of RAlO_3 were obtained from Shishido *et al.* (3).

REFERENCES

1. S. Geller and V. B. Bala, *Acta Crystallogr.* **9**, 1019 (1956).
2. D. Dernier and R. G. Maines, *Mater. Res. Bull.* **6**, 433 (1971).
3. T. Shishido, S. Nojima, M. Tanaka, H. Horiuchi, and T. Fukuda, *J. Alloys Compounds* **227**, 175 (1995).
4. T. Shishido, A. Yoshikawa, H. Horiuchi, and T. Fukuda, *J. Chem. Soc. Jpn: Chem. Ind. Chem.* **7**, 573 (1995).
5. W. H. Zachariasen, *Acta Crystallogr.* **2**, 388 (1949).
6. T. Shishido, M. Tanaka, H. Horiuchi, and T. Fukuda, *Chem. Soc. Jpn: Chem. Ind. Chem.* **6**, 680 (1992).
7. M. Tanaka, T. Shishido, H. Horiuchi, N. Toyota, D. Shindo, and T. Fukuda, *J. Alloys Compounds* **192**, 87 (1993).
8. S. Nakagawa, T. Shishido, M. Tanaka, S. Nojima, H. Horiuchi, and T. Fukuda, *Chem. Soc. Jpn: Chem. Ind. Chem.* **8**, 752 (1994).
9. Y. S. Kim, *Acta Crystallogr., B* **24**, 295 (1968).
10. H. Toraya, *J. Appl. Crystallogr.* **19**, 440 (1986).
11. C. W. Burnham, *Carnegie Inst. Washington Year Book.* **61**, 132 (1962).
12. R. D. Shannon and C. T. Prewitt, *Acta Crystallogr. B* **25**, 925 (1969).
13. H. M. O'Bryan, P. K. Gallaher, G. W. Berkstresser, and C. D. Brandle, *J. Mater. Res.* **5**, 183 (1990).